Proceedings of the 8th International Conference on Pedestrian and Evacuation Dynamics (PED2016)
Hefei, China - Oct 17 – 21, 2016
Paper No. 1

Influences of Extraction Techniques on the Quality of Measured Quantities of Pedestrian Characteristics

Maik Boltes [1] Stefan Holl [1] Antoine Tordeux [1] Armin Seyfried [1] Andreas Schadschneider [2] and Ulrich Lang [3]

[1] *Jülich Supercomputing Centre, Forschungszentrum Jülich, Germany*
{*m.boltes, st.holl, a.tordeux, a.seyfried*}*@fz-juelich.de*
[2] *Institut für Theoretische Physik, Universität zu Köln, Germany*
[3] *Institut für Informatik, Universität zu Köln, Germany*

Abstract - For the proper understanding and modelling of pedestrian dynamics, reliable empirical data are necessary. Trajectories of every person with a high temporal and spatial resolution allow a detailed analysis of movement as well as the calibration and verification of microscopic models in space and time.

To extract individual trajectories on a microscopic level different techniques have been developed depending on miscellaneous requirements. In this paper we analyse how the quality of quantities like velocity or density depend on the technique chosen to track pedestrians. For this purpose, errors due to perspective distortion, use of markers, type of markers, and other conditions will be scrutinized.

It turns out that the usage of imaging systems like cameras give currently the best results and that marker particularly structured marker for detecting a person in a crowd obtain the most accurate trajectory especially if the height of the person is coded by the marker or the distance to the camera is measured otherwise. To minimize the errors resulting from the perspective view a small angle of view and thus high mounted cameras should be used for capturing the whole area of interest. The small angle of view also decreases the risk of occlusion and lens systems for large focal lengths usually have a smaller optical distortion error.

Keywords: Experiments; trajectories; extraction; measurement error

1. Introduction

To understand and to model pedestrian dynamics reliable empirical data is needed. Collecting the trajectories of every person with a high temporal and spatial resolution allows a detailed analysis of movement and the calibration and verification of microscopic models in space and time [1].

The level of detail of the extracted information varies. For getting an impression of the overall movement of a crowd, determining abnormal behaviour or separating the crowd in areas of different activity the optical flow can help [2–4]. Also the calculation of the velocity in a certain area is possible without detecting single pedestrians. An estimation of the density is feasible as well [5].

A high level of detail detects and tracks the skeleton of a person. First studies analyzing precise motion sequences already started with the chronophotography in the 19th century [6]. Today the Microsoft Kinect for gaming or motion capturing systems in film productions for steering virtual characters are able to do the skeletal detection and tracking automatically in real-time [7].

For the analysis of peoples' motion the highest possible level would be the best, but for crowds with high density no system is able to track the full locomotion system. And up to now most of the models simulating pedestrian dynamics do not consider the motion of all parts of a body, although taking, for example, the gait into account may enhance the quality of the simulation results [8].

Thus most data provided for analysis and model pedestrian dynamics are trajectories of every single pedestrian, sometimes enriched with some additional global (e. g., distribution of age and gender) or individual (e. g., body size, head or shoulder orientation) information. The set of trajectories of all pedestrians provides data like velocity, flow, density and individual distances at any time and position, thus lane formation and local densities can be analyzed [9]. Different techniques have been developed to extract individual trajectories on a microscopic level depending on miscellaneous requirements [10].

Fig. 1: Observations with extracted trajectories of pedestrians in field studies, and laboratory experiments using colored caps or black dot markers. The determined position is encircled in blue, and the red path is the way of every person in the last second.

In our experience, some of the contradictions in the literature can be traced back to insufficient methods of data capturing or inadequate resolution of the measurement in time and space [11]. This paper discusses how the quality of quantities like velocity or density depend on the technique chosen to track pedestrians. For this purpose, measurement errors due to perspective distortion, use of markers, type of markers, and other conditions will be scrutinized.

2. Extraction techniques

For the extraction of trajectories different techniques have been developed. To perform field studies methods have to be chosen without intervention and preparation of the observed people. These methods often also have to get along with the restriction having to work in real-time (e. g., for privacy protection) and using already installed surveillance cameras with a slanted viewing angle (large observation space, but high occlusion level). To detect individual persons in crowds monocular cameras [12], stereo cameras [13, 14], multi camera systems [15], near-infrared cameras [16], thermographic cameras [17], RGB-D sensors [18, 19] or time-of-flight cameras [20] have been used. Also other systems exist, but according to Teixeira [21] the best modality across the board for detection and tracking of people is vision (i.e. cameras and other imagers) and computer vision is far ahead from other instrumented modalities especially with respect to spatial-resolution and precision metrics. Nevertheless Dollar stated in [22] that also under favorable conditions with pedestrians at least 80 pixels tall, 20–30 % of all pedestrians are missed with at most one false alarm every ten images. Also Nguyen writes in 2015 [12] that effective detectors can only be constructed for applications where a full upright body is visible or a upper body with less deformation. All camera systems have in common that the detection error increases with increasing density.

Prior information helps to enhance the detection rate. For laboratory experiments one is able to mark the participants, thus most of the researchers collecting data from these experiments use utilities to ease the detection. Figure 1 shows three types of observations in field studies and laboratory experiments, where the detected position of every pedestrian is encircled in blue while red paths show the position of the last second. The most common way of marker are colored caps [23–33]. Others use structured marker, e. g., for indicating the head [34, 35] or the shoulder direction [36] or code additional information [37–40] for a more precise trajectory [41, 42].

For crowds the viewing angle should be as perpendicular as possible to have minimal occlusion for small focal lengths. From the people only the head or at most the shoulders are visible and thus can be detected The trajectories of people tracked in that way describe the path of the head including the swaying and not the center of mass. Later smoothing of the resulting trajectories is possible [43].

3. Measurement errors

The measurement errors made during the detection of people's position can be differentiated between these types:

1. Detection: too many or too few detected persons
2. Position: systematical error depending on the distance to the image center:
   (a) Increasing error of the position (possible reason: quality of undistortion, marker type)

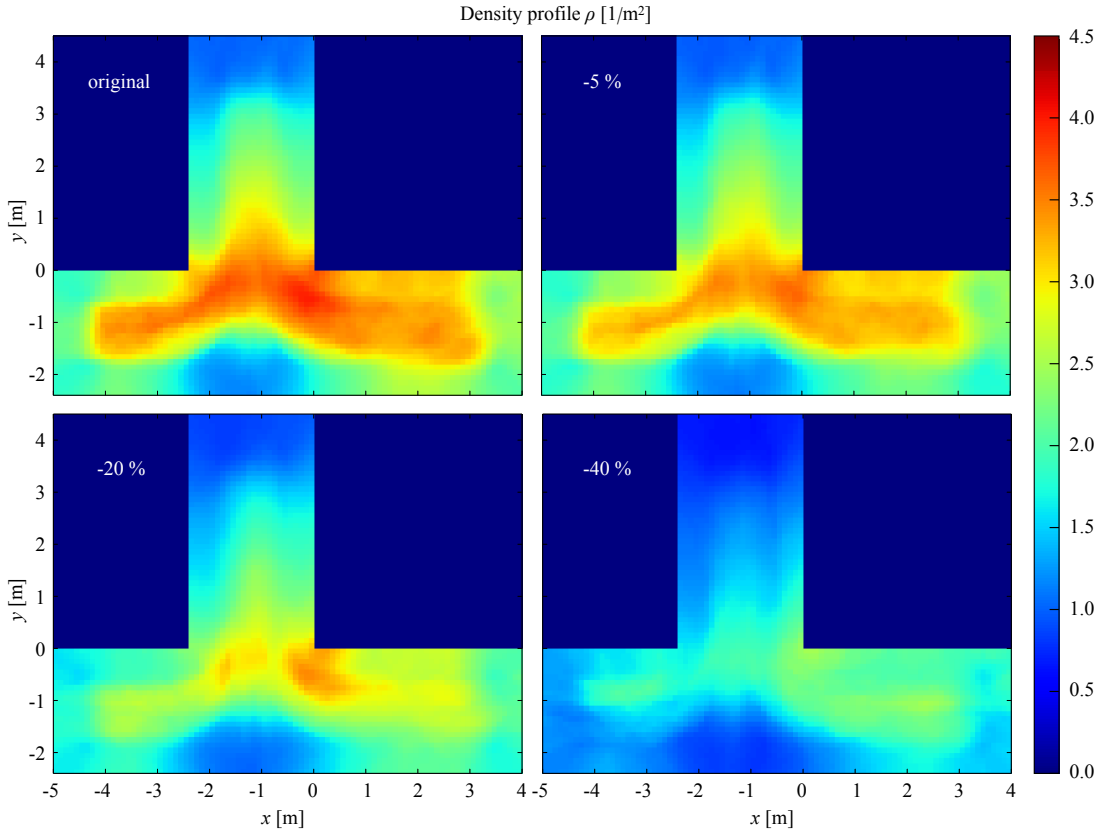

Fig. 2: Density profiles of an experiment at a T-junction with increasing false-negative-rate of 5 %, 20 % and 40 %. The density decreases linearly to the false-negative-rate.

(b) Increasing error variance of the position (possible reason: uncertainty in persons' height)

3. Position: local error (possible reason: varying detected position of the head)

These errors have different influences on quantities used for analysing pedestrian dynamics.

3.1. Detection error

For laboratory experiments the error type 1 of missing or surplus detections should be negligible, if the experiment is reasonably conducted. Otherwise it should be possible to delete false positive detections and add false negative misses so that subsequent steps of analysis do not lead to wrong implications. Figure 2 shows the impact of the false-negative-rate to the density by the example of an experiment at a T-junction [42]. The profiles have been calculated using the Voronoi method [43]. With increasing false-negative-rate the density decreases substantially. The correct average density is $2.47/\mathrm{m}^2 \pm 0.76/\mathrm{m}^2$. The density decreases for a false-negative-rate of 5 %, 20 % and 40 % to $2.31/\mathrm{m}^2 \pm 0.70/\mathrm{m}^2$ (about 94 % of the original), $2.00/\mathrm{m}^2 \pm 0.61/\mathrm{m}^2$ (about 81 % of the original) and $1.48/\mathrm{m}^2 \pm 0.46/\mathrm{m}^2$ (about 60 % of the original) respectively. The density just as the flow decreases proportional to the false-negative-rate, thus a false-negative-rate of 20 % for the best results and under best conditions of the markerless methods as described in the previous section will lead to a density and flow of 80 % of the original value. This yields to the outcome that general markerless extraction techniques without optimization to the observed scene and without subsequent error correction are not applicable for a detailed analysis of the dynamic inside a crowd.

3.2. Systematic error of the position caused by insufficient calibration

To extract a real metric position from a raster graphics image an intrinsic and extrinsic calibration have to be performed. The intrinsic calibration determines camera parameters like focal length and principal point and nonlinear parameters describing the lens distortion. This camera resectioning uses only a model that never fits perfectly the real distortion of a lens system. The extrinsic calibration

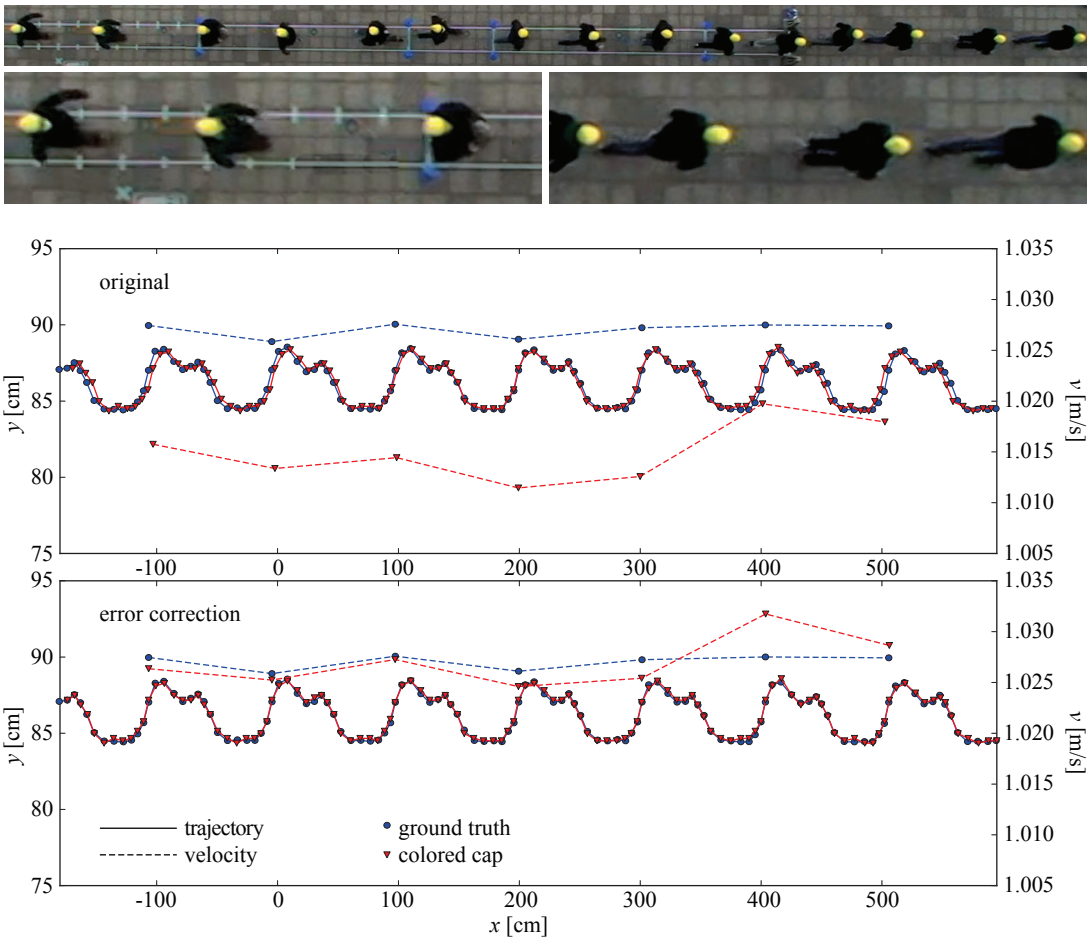

Fig. 3: Top: people with colored caps walking below a camera. The cap on the left is seen from the front and on the right from the back (magnification of the outer part in the second row). Middle: trajectory of a virtual person detected by a worn colored cap (red) and the true path of that person (blue). The derived velocity differs up to 0.015 m/s (1.5 %). Bottom: corrected trajectory and the corresponding velocities.

calculates the position and the heading of the camera in real world. After both calibrations the combined error e_c can be determined by reprojection. To quantify this error, which leads to an incorrect position of a detected person, one needs real 3D positions and corresponding pixel coordinates. These pairs of coordinates should be chosen within the experimental setup in areas, where the position of the people are extracted. Caused by the structure of the lens systems these errors increase from the image center to the image border and edges especially for often used wide angle lenses. For the latest experiments performed from Forschungszentrum Jülich a GoPro HERO4 Black Edition camera and a camera model with radial distortion parameters up to the order of six was used. The average pixel error for a maximum viewing angle of 52° was 2.2 pixel (maximum 6.4 pixel), which leads to an average metric error of 0.011 m (maximum 0.035 m) at an average distance to the heads of 3.8 m for this experimental setup. Since the determination of the 3D position was done by a leveling pole holding by hand the small error can also be influenced by the measuring technique.

3.3. Systematic error of the position caused by colored caps marker

A second systematical error which depends on the distance to the image center bases on the used marker type. As described in Section 2 the most used marker type are colored caps. They are easy to segment in the image and can be bought without additional work of preparation. Seldom described in the papers in detail, but one can suppose that the adopted position of a person is the geometric center of the color segment of his cap.

Figure 3 shows the problem with this approach. Depending on the angle at which the cap is seen by the perspective view of the camera the resulting geometric center of the color segment belongs to different positions on the head of the person. For a perpendicular view of the camera people moving towards the

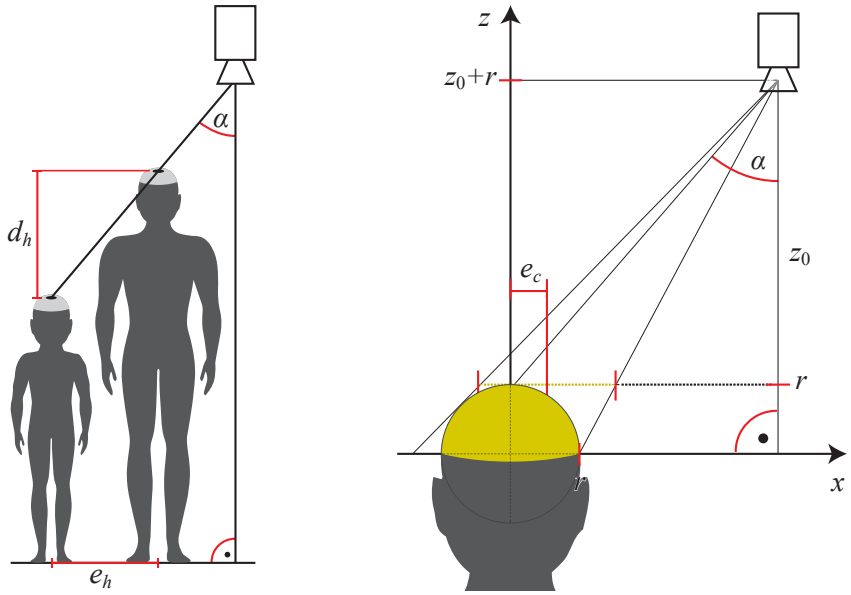

Fig. 4: Left: the same pixel in a perspective camera image corresponds to different positions on the ground plane due to differing heights of the persons. Right: the geometric center of the segment of an idealized colored cap as hemisphere in a perspective image is shifted by e_c to the center of the head.

image center are seen from the front and people moving from the image center to the border are seen more and more from the back. This leads to a systematic shift of the position to the image center and thus, e. g., an underestimation of the velocity of a person. In the bottom of Figure 3 the trajectory and the velocity for a virtual person is shown. The red lines result from the center of a colored cap and the blue lines are the ground truth.

For an idealized colored cap as hemisphere the right of Figure 4 sketches the position error e_m due to the viewing angle α and distance to the camera z_0 with an assumed head radius of r. The position error is

$$e_m = \frac{r}{2}\left(\frac{z_0 + z_0\tan\alpha}{z_0 + r} + \frac{\sin\left(\arcsin\frac{r}{\sqrt{(z_0\tan\alpha)^2+(z_0+r)^2}} + \arctan\frac{z_0\tan\alpha}{z_0+r}\right) - 1}{\cos\left(\arcsin\frac{r}{\sqrt{(z_0\tan\alpha)^2+(z_0+r)^2}} + \arctan\frac{z_0\tan\alpha}{z_0+r}\right)}\right). \tag{1}$$

For typical distances z_0 larger than 2 m z_0 can be neglected. With a head radius of 0.07 m (frontal view) the error can be estimated by the linear function

$$e_m \approx \alpha \cdot 0.0012\,\mathrm{m}/^\circ\,. \tag{2}$$

A detailed description can be found in [44].

Applying Equation 2 to the trajectory of the virtual person in Figure 3 the corrected position fits very good to the ground truth and thus the error of 0.015 m/s (1.5 %) of the derived velocity is almost eliminated.

Structured marker like caps with a black dot, where the dot is always visible and used for determining the position, have no systematic error caused by the marker, because in every frame the same object on the head is localized [42].

3.4. Systematic error variance of the position caused by wrong persons' height

The perspective view of a camera and its perspective distortion leads to an error of the position, if the distance between the detected head and the camera or the height of the person for plane experiments respectively is not known. A pixel in the image may correspond to different heights at different positions on the ground plane as illustrated on the left of Figure 4. An average height could be chosen, but produces an error e_h of the position on the ground plane of

$$e_h = |d_h \tan\alpha| \tag{3}$$

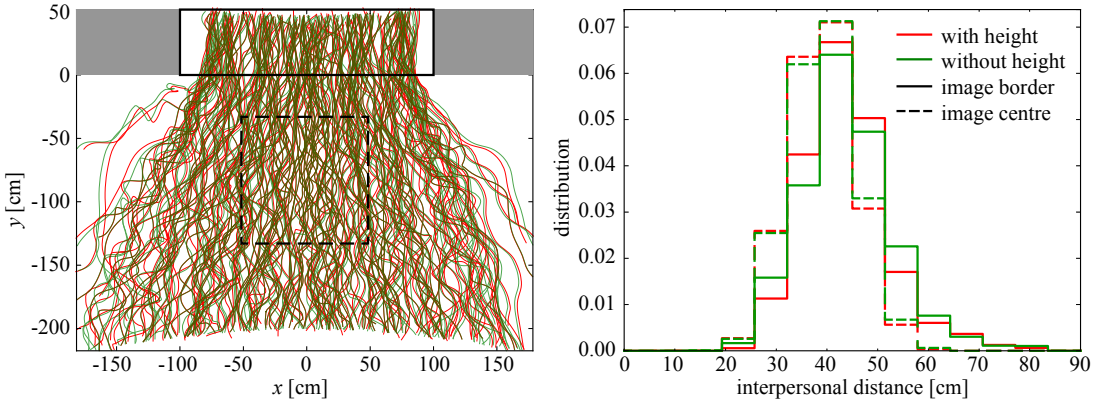

Fig. 5: Left: trajectories of a bottleneck experiment with considered height (red) and without (green). Right: distribution of the interpersonal distance for the dashed area in the center of the image and the framed region at the top of the image. The variance increases at the image border, if the height of the persons is neglected.

for a viewing angle α and a height difference d_h. The error variance of the position increases from the image center to the border of the image. For instance for a wide angle lens with an angle of view of 70° and participants with heights between 1.6 m and 2.0 m the maximum error at the border is

$$e_h = \left| \frac{2.0\,\mathrm{m} - 1.6\,\mathrm{m}}{2} \tan\frac{70^\circ}{2} \right| \approx 0.14\,\mathrm{m}\,, \tag{4}$$

if an average height of 1.8 m is chosen for the calculation of the position.

To decrease this error one can use marker coding the height [34] or use techniques to measure the distance between the camera and the head. With systems which are able to determine the 3D position of an object (stereo cameras, multi camera systems, RGB-D sensors, time-of-flight cameras) the systematic error caused by the perspective distortion can be minimized to the accuracy of the chosen system. These systems also allow experiments at stairs or ramps with resulting 3D trajectories [13].

To show the influence of this error to the analysis of pedestrian dynamics Figure 5 presents the measured interpersonal distance, which is often used for identifying the neighbors of a person or study the proxemic. In Figure 5 for the red trajectories the height of the persons is used, contrary to the green trajectories, where an average height is chosen for all persons. In the image center (dashed area) the error due to the neglected height is insignificant. At the border, for the example at the top framed region, the error increases and leads to a larger variance of the interpersonal distance. On the left and right the different positions of corresponding trajectories are well visible.

3.5. Local position error

If the detected position on the head of a person along a trajectory is not the same a jitter along the path can be observed. This phenomena can slightly be seen on the left of Figure 1, where the position is determined by an extraction method without marker [42]. To quantify the smoothness the average microscopic acceleration can be used. For successive detected points, $p_i(t_j)$, along a trajectory of person i in a uniform image sequence of length N the microscopic acceleration at time $t_j \in \{t_j | j \in \mathbb{N}_N\}$ is

$$a_i(t_j) = \frac{\|(p_i(t_{j+1}) - p_i(t_j)) - (p_i(t_j) - p_i(t_{j-1}))\|}{(t_{j+1} - t_j)^2}\,. \tag{5}$$

The acceleration is called microscopic, because the evaluation is done along the trajectory and not along the main moving direction.

Also the normal movement of a person causes an acceleration. This normal acceleration can be measured by using structured marker for which the same position on the head is chosen in every frame. Thus the ground truth of the acceleration for walking people in a crowd is $1.2\,\mathrm{m/s^2} \pm 0.7\,\mathrm{m/s^2}$. For a markerless technique using a stereo camera [42] the microscopic acceleration is $6.5\,\mathrm{m/s^2} \pm 6.8\,\mathrm{m/s^2}$. But also, if colored caps are chosen for detecting successive positions of the persons along their path, the detected locations are less stable and thus the acceleration increases, because pixel belonging to the cap change due to the material of the cap and varying illumination and incidence angle along a path over the area of the experiment. The observed acceleration is $2.5\,\mathrm{m/s^2} \pm 1.7\,\mathrm{m/s^2}$. All values have been calculated

for the same experiment (T-junction with two merging streams visible on the right of Figure 1), but with neglected black dot for imitating a colored cap and without taking the cap into account for the markerless technique.

The varying detected position of the head has an influence on all quantities describing pedestrian dynamics, e. g., the jitter leads to a less prominent visibility of lane formations along a corridor.

4. Conclusion

Trajectories of individual pedestrians are used to analyze the dynamics between pedestrians. This paper gave a summery of errors resulting from the used extraction technique (markerless, colored caps, structured marker). The errors have an influence on the derived quantities describing pedestrian dynamics, which has been shown by example.

The maximum assumable error is the superposition of all maximum errors, because the errors are independent. For the experiment in Section 3.2 and the supposed height difference of Section 3.4 the three systematical errors result in a combined maximum error at the border of

$$\begin{aligned} e_c + e_m + e_h &\approx 0.035\,\mathrm{m} + 52^\circ \cdot 0.0012\,\mathrm{m}/^\circ + 0.2\,\mathrm{m} \cdot \tan 52^\circ \\ &\approx 0.035\,\mathrm{m} + 0.062\,\mathrm{m} + 0.256\,\mathrm{m} \\ &= 0.353\,\mathrm{m}\,. \end{aligned} \tag{6}$$

A structured marker obtains the most accurate trajectory ($e_m \approx 0\,\mathrm{m}$) especially if the height of the person is coded by the marker ($e_h \ll 0.256\,\mathrm{m}$) [34]. The distance to the camera can also be measured by special equipment to reduce the systematic error variance caused by incorrect persons' height and to get the opportunity to gather trajectories in 3D like at stairs or ramps [13].

To minimize the errors resulting from the perspective view like the error due to neglecting the individual height and the error according to the taken marker one should use small angle of view and thus high mounted cameras to capture the whole experimental area. The small angle of view also decreases the risk of occlusion and lens systems for large focal lengths generally have a smaller optical distortion error, which are easier to reproduce by a camera model used for undistortion.

Sometimes the area to be observed is to large for one camera, especially if the ceiling height is low so that trajectories of different overlapping camera views have to be merged. Then all mentioned errors have an influence of the closeness of the trajectories which belong to the same person, in particular because the overlapping area is typically at the border of the images. The accuracy of detected positions of a trajectory are more accurate, the position is nearer to the image center.

To summarize, we would suggest to use structured marker captured by a system with a large focal lens and a possibility to measure the distance to the camera to get the smallest possible error. While extracting and further usage of trajectories the inherent errors should be taken into account and while publishing the results the error should be quantified and specified.

References

[1] Steffen, B., Seyfried, A., Boltes, M.: Reliability issues in the microscopic modeling of pedestrian movement. In: H.K. Pavel Exner (ed.) Mathematical results in Quantum Physics, pp. 254–259 (2011)

[2] Krausz, B., Bauckhage, C.: Loveparade 2010: Automatic video analysis of a crowd disaster. Computer Vision and Image Understanding, Special issue on Semantic Understanding of Human Behaviors in Image Sequences **116**(3), 307–319 (2012)

[3] Ali, S., Shah, M.: A lagrangian particle dynamics approach for crowd flow segmentation and stability analysis. In: Conference on Computer Vision and Pattern Recognition, pp. 1–6 (2007)

[4] Pathan, S.S., Richter, K.: Pedestrian behavior analysis with image-based method in crowds. In: Traffic and Granular Flow 2013, pp. 187–194 (2015)

[5] Ryan, D., Denman, S., Sridharan, S., Fookes, C.: An evaluation of crowd counting methods, features and regression models. Computer Vision and Image Understanding **130**, 1–17 (2014)

[6] Muybridge, E.: Animal locomotion, Plate 519 (1887)

[7] Gmiterko, A., Liptak, T.: Motion capture of human for interaction with service robot. American Journal of Mechanical Engineering **1**(7), 212–216 (2013)

[8] Chraibi, M., Seyfried, A., Schadschneider, A.: Generalized centrifugal force model for pedestrian dynamics. Physical Review E **82**, 046111 (2010)

[9] Liddle, J., Seyfried, A., Steffen, B.: Analysis of bottleneck motion using Voronoi diagrams. In: Peacock et al. [45], pp. 833–836

[10] Boltes, M., Seyfried, A.: Collecting Pedestrian Trajectories. Neurocomputing, Special Issue on Behaviours in Video **100**, 127–133 (2013)

[11] Seyfried, A., Boltes, M., Kähler, J., Klingsch, W., Portz, A., Rupprecht, T., Schadschneider, A., Steffen, B., Winkens, A.: Enhanced empirical data for the fundamental diagram and the flow through bottlenecks. In: Klingsch et al. [46], pp. 145–156

[12] Nguyen, D.T., Li, W., Ogunbona, P.O.: Human detection from images and videos: A survey. Pattern Recognition pp. 148–175 (2015)

[13] Boltes, M., Seyfried, A., Steffen, B., Schadschneider, A.: Using Stereo Recordings to Extract Pedestrian Trajectories Automatically in Space. In: Peacock et al. [45], pp. 751–754

[14] van Oosterhout, T., Englebienne, G., Kröse, B.: Rare: people detection in crowded passages by range image reconstruction. Machine Vision and Applications pp. 1–13 (2015)

[15] Kiss, Á., Szirányi, T.: Localizing people in multi-view environment using height map reconstruction in real-time. Pattern Recognition Letters **34**(16), 2135–2143 (2013)

[16] Hadi, H.S., Rosbi, M., Sheikh, U.U.: A review of infrared spectrum in human detection for surveillance systems. International Journal Of Interactive Digital Media **1**(3), 13–20 (2013)

[17] Saito, H., Hagihara, T., Hatanaka, K., Sawai, T.: Development of pedestrian detection system using far-infrared ray camera. Sei Technical Review **66**, 112–117 (2008)

[18] Jafari, O.H., Mitzel, D., Leibe, B.: Real-time rgb-d based people detection and tracking for mobile robots and head-worn cameras. In: IEEE International Conference on Robotics and Automation (ICRA) (2014)

[19] Corbetta, A., Bruno, L., Muntean, A., Toschi, F.: High statistics measurements of pedestrian dynamics. Transportation Research Procedia **2**, 96–104 (2014)

[20] Benedek, C.: 3d people surveillance on range data sequences of a rotating lidar. Pattern Recognition Letters, Special Issue on Depth Image Analysis (2014)

[21] Teixeira, T., Dublon, G., Savvides, A.: A survey of human-sensing: Methods for detecting presence, count, location, track, and identity. ACM Computing Surveys **5**(1) (2010)

[22] Dollár, P., Wojek, C., Schiele, B., Perona, P.: Pedestrian detection: An evaluation of the state of the art. Pattern Analysis and Machine Intelligence, IEEE Transactions on **34**(4), 743–761 (2012)

[23] Hoogendoorn, S., Daamen, W., Bovy, P.: Extracting microscopic pedestrian characteristics from video data. In: TRB2003 Annual Meeting (2003)

[24] Daamen, W., Hoogendoorn, S.: Capacity of doors during evacuation conditions. Procedia Engineering, 1st Conference on Evacuation Modeling and Management **3**(0), 53–66 (2010)

[25] Liu, X., Song, W., Zhang, J.: Extraction and quantitative analysis of microscopic evacuation characteristics based on digital image processing. Physica A: Statistical Mechanics and its Applications **388**(13), 2717–2726 (2009)

[26] Tian, W., Song, W., Ma, J., Fang, Z., Seyfried, A., Liddle, J.: Experimental study of pedestrian behaviors in a corridor based on digital image processing. Fire Safety Journal **47**(0), 8–15 (2012)

[27] Saadat, S., Teknomo, K.: Automation of pedestrian tracking in a crowded situation. In: R.D. Peacock, E.D. Kuligowski, J.D. Averill (eds.) Pedestrian and Evacuation Dynamics, pp. 231–239 (2011)

[28] Wong, S.C., Leung, W.L., Chan, S.H., Lam, W.H.K., Yung, N.H.C., Liu, C.Y., Zhang, P.: Bidirectional Pedestrian Stream Model with Oblique Intersecting Angle. Journal of Transportation Engineering **136**(3), 234–242 (2010)

[29] Shiwakoti, N., Shi, X., Zhirui, Y., Wang, W.: Empirical study on pedestrian crowd behaviour in right angled junction. In: 37th Australasian Transport Research Forum (ATRF) (2015)

[30] Lian, L., Mai, X., Song, W., Kit, Y.K.: An experimental study on four-directional intersecting pedestrian flows. J. Stat. Mech p. P08024 (2015)

[31] Liu, X., Song, W., Fu, L., Fang, Z.: Experimental study of pedestrian inflow in a room with a separate entrance and exit. Physica A: Statistical Mechanics and its Applications **442**, 224–238 (2016)

[32] Shiwakoti, N., Gong, Y., Shi, X., Ye, Z.: Examining influence of merging architectural features on pedestrian crowd movement. Safety Science **75**, 15–22 (2015)

[33] Tomoeda, A., Yanagisawa, D., Nishinari, K.: Escape velocity of the leader in a queue of pedestrians. In: Traffic and Granular Flow 2013, pp. 213–218 (2015)

[34] Boltes, M., Seyfried, A., Steffen, B., Schadschneider, A.: Automatic Extraction of Pedestrian Trajectories from Video Recordings. In: Klingsch et al. [46], pp. 43–54

[35] Ezaki, T., Ohtsuka, K., Chraibi, M., Boltes, M., Yanagisawa, D., Seyfried, A., Schadschneider, A., Nishinari, K.: Inflow process of pedestrians to a confined space. submitted to Collective Dynamics

[36] Lemercier, S., Moreau, M., Moussaïd, M., Theraulaz, G., Donikian, S., Pettré, J.: Reconstructing motion capture data for human crowd study. In: J. Allbeck, P. Faloutsos (eds.) Motion in Games, *Lecture Notes in Computer Science*, vol. 7060, pp. 365–376 (2011)

[37] Mehner, W., Boltes, M., Mathias, M., Leibe, B.: Robust marker-based tracking for measuring crowd dynamics. In: L. Nalpantidis, V. Krüger, J.O. Eklundh, A. Gasteratos (eds.) Computer Vision Systems, from International Conference on Computer Vision Systems (ICVS), *Lecture Notes in Computer Science*, vol. 9163, pp. 445–455 (2015)

[38] Mehner, W., Boltes, M., Seyfried, A.: Methodology for generating individualized trajectories from experiments. In: Traffic and Granular Flow 2015 (2015)

[39] Stuart, D., Christensen, K.M., Chen, A., Kim, Y., Chen, Y.: Utilizing augmented reality technology for crowd pedestrian analysis involving individuals with disabilities. In: Proceedings of the ASME International Design Engineering Technical Conferences & Computers and Information in Engineering Conference (2013)

[40] Bukáček, M., Hrabák, P., Krbálek, M.: Experimental study of phase transition in pedestrian flow. Transportation Research Procedia **2**(0), 105–113 (2014)

[41] Bukáček, M., Hrabák, P., Krbálek, M.: Experimental analysis of two-dimensional pedestrian flow in front of the bottleneck – experimental analysis of 2d pedestrian flow. In: Traffic and Granular Flow 2013, pp. 93–101 (2015)

[42] Boltes, M., Zhang, J., Seyfried, A., Steffen, B.: T-junction: Experiments, trajectory collection, and analysis. In: IEEE International Conference on Computer Vision Workshop on Modeling, Simulation and Visual Analysis of Large Crowds, pp. 158–165 (2011)

[43] Steffen, B., Seyfried, A.: Methods for measuring pedestrian density, flow, speed and direction with minimal scatter. Physica A **389**(9), 1902–1910 (2010)

[44] Boltes, M.: Automatische Erfassung präziser Trajektorien in Personenströmen hoher Dichte. Hochschulschrift (dissertation), Mathematisch-Naturwissenschaftliche Fakultät der Universität zu Köln (2015)

[45] Peacock, R.D., Kuligowski, E.D., Averill, J.D. (eds.): Pedestrian and Evacuation Dynamics 2010 (2011)

[46] Klingsch, W.W.F., Rogsch, C., Schadschneider, A., Schreckenberg, M. (eds.): Pedestrian and Evacuation Dynamics 2008 (2010)